

## *Ab Initio* Investigation of Collective Charge Excitations in MgB<sub>2</sub>

Wei Ku,<sup>1</sup> W. E. Pickett,<sup>1</sup> R. T. Scalettar,<sup>1</sup> and A. G. Eguiluz<sup>2</sup>

<sup>1</sup>*Physics Department, University of California, Davis, California 95616*

<sup>2</sup>*Department of Physics and Astronomy, The University of Tennessee, Knoxville, Tennessee 37996-1200  
and Solid State Division, Oak Ridge National Laboratory, Oak Ridge, Tennessee 37831-6030*

(Received 18 May 2001; published 16 January 2002)

A sharp collective charge excitation is predicted in MgB<sub>2</sub> at  $\sim 2.5$  eV for  $q$  perpendicular to the boron layers, based on an all-electron analysis of the dynamical density response within time-dependent density functional theory. This novel excitation, consisting of coherent charge fluctuation between Mg and B sheets, induces an abrupt plasma edge in the experimentally observable reflectivity. The existence of this mode reflects the unique electronic structure of MgB<sub>2</sub> that is also responsible for strong electron-phonon coupling. By contrast, the acoustic plasmon, recently suggested to explain the high  $T_c$ , is not realized when realistic transition strengths are incorporated.

DOI: 10.1103/PhysRevLett.88.057001

PACS numbers: 74.70.Ad, 78.20.Bh

The high critical temperature,  $T_c \sim 40$  K, of the newly discovered [1] conventional superconductor MgB<sub>2</sub> has attracted much attention [2–9]. A consistent picture within BCS theory [10–12] seems to be given by the qualitative analysis [2,3] based on the large hole density of states at the Fermi surface, provided by the boron  $\sigma$  bands. On the other hand, other possible contributions to pairing [7,8,13] have not been totally ruled out, since a quantitative analysis of  $T_c$ , via realistic treatment of screened electron-electron and electron-phonon interactions [4], has yet to be performed. The insight into the behavior of the cuprate superconductors resulting from consideration of the spin susceptibility suggests that it might be especially interesting to examine the possibility of unusual collective charge excitations in MgB<sub>2</sub> with such realistic treatments. In particular, a calculation of the dynamical density response would give detailed information on electronic excitations, which control most of the macroscopic properties, including the dielectric function and thereby superconductivity [12].

Even within phonon-mediated theories, there currently exists large speculation on the value of the Coulomb pseudopotential  $\mu^*$ , from 0.02 to 1 [5,6]. An intriguing proposal [5] has recently suggested that an anomalously small  $\mu^*$  may originate from the existence of an acoustic plasmon (AP) [14,15], which develops from two characteristic charge carriers in MgB<sub>2</sub>: “heavy” holes of B  $\sigma$  bands and “light” electrons and holes of B  $\pi$  bands. This is an important issue, as the existence of an AP can drastically alter the dynamical electronic screening and may even provide an additional pairing channel [15]. Thus, it is vital to reexamine the existing tight-binding result via a more realistic investigation that takes effects of the crystal potential fully into account.

In this Letter we present results of an *ab initio*, all-electron, calculation of the dynamical density-response function of MgB<sub>2</sub> within the framework of time-dependent density functional theory (TDDFT) [16]. Our key result is the prediction of a sharp collective mode whose origin

is the strong coherent charge fluctuation between parallel sheets of B and Mg. This novel charge excitation, found to reside within the [0002] zone-boundary gap, embodies a remarkable signature of the electronic structure of MgB<sub>2</sub>, and results in a dramatic change in the reflectivity near 2.5 eV for  $q$  perpendicular to the boron layers. It thus explains naturally the strong increase in the Raman efficiency reported very recently [9]. The impact of this mode on the Coulomb pseudopotential will be briefly addressed. In addition, with the matrix elements that control the transition probability fully included, the recently proposed acoustic plasmon is not realized in our results, as a consequence of weak intraband transition of the “heavy carriers.” Finally, comments on the proposed two-band-type superconducting instabilities will be given to further illustrate the importance of including realistic transition strengths.

Within TDDFT, the dynamical density response function  $\chi(\vec{x}, t; \vec{x}', t') = \delta\rho(\vec{x}, t)/\delta v_{ext}(\vec{x}', t')$  with density  $\rho$  and external potential  $v_{ext}$  can be obtained through the following integral equation [16]:

$$\chi = \chi^{KS} + \chi^{KS}(v + f_{xc})\chi, \quad (1)$$

where  $\chi^{KS}(\vec{x}, t; \vec{x}', t')$  is the response function for “non-interacting” Kohn-Sham (KS) electrons,  $v(\vec{x} - \vec{x}')$  is the Coulomb interaction, and  $f_{xc}(\vec{x}, t; \vec{x}', t') = \delta v_{xc}(\vec{x}, t)/\delta\rho(\vec{x}', t')$  accounts for dynamical exchange-correlation effects (where  $v_{xc}$  is the time-dependent exchange-correlation potential in TDDFT). Working in Fourier space,  $\chi^{KS}$  can be calculated with the KS eigenenergies,  $\epsilon_{\vec{k}, n}$ , and the corresponding eigenstates,  $|\vec{k}, n\rangle$ , of the ground state [17]:

$$\begin{aligned} \chi_{\vec{G}, \vec{G}'}^{KS}(\vec{q}, \omega) = & \frac{1}{V} \sum_{\vec{k}}^{\text{BZ}} \sum_{n, n'} \frac{f_{\vec{k}, n} - f_{\vec{k}+\vec{q}, n'}}{\epsilon_{\vec{k}, n} - \epsilon_{\vec{k}+\vec{q}, n'} + \hbar(\omega + i0^+)} \\ & \times \langle \vec{k}, n | e^{-i(\vec{q}+\vec{G})\cdot\vec{x}} | \vec{k} + \vec{q}, n' \rangle \\ & \times \langle \vec{k} + \vec{q}, n' | e^{i(\vec{q}+\vec{G}')\cdot\vec{x}} | \vec{k}, n \rangle, \end{aligned} \quad (2)$$

where  $\vec{G}$  is a vector of the reciprocal lattice,  $n$  is a band index, the wave vectors  $\vec{k}$  and  $\vec{q}$  are in the first Brillouin

zone, and  $V$  is the normalization volume. Equation (1) is then numerically solved as a matrix equation [18].

We stress that this formalism is rigorous. Even though a formal connection between the KS eigenenergies and the quasiparticle energies has not been established, the physical meaning of the KS band structure (including the empty states) is to be realized through its contribution to the density fluctuation in  $\chi^{\text{KS}}$ . The only physical approximation introduced in this work is the functional form of  $v_{xc}(\vec{x}, t)$ , for which the adiabatic local density approximation (ALDA) [16] is chosen. Since only the long wavelength limit is of interest in the present work, we further drop  $f_{xc}$  from Eq. (1), as its strength (within ALDA) cannot compete with the singular  $v$  without sizable crystal local-field effects [18]. In this limit, the dielectric function  $\epsilon = (1 + v\chi)^{-1}$  can be visualized directly from the single-particle transitions of the KS particles, with the relation  $\epsilon = 1 - v\chi^{\text{KS}}$ .

Numerically, in order to resolve the features in the narrow energy range where the AP may occur, the broadening parameter, commonly employed [19] in place of  $0^+$  in Eq. (2), needs to be very small ( $\sim 10$  meV). This in turn requires a dense  $k$  mesh, to carefully sample the momentum-energy phase space near the Fermi surface. The results presented in this work correspond to a uniform mesh of  $20 \times 20 \times 60$ . In addition, summing the narrow  $\delta$  functions is avoided by first evaluating Eq. (2) on the imaginary frequency axis, followed by analytic continuation via Padé approximants [20].

The calculated dielectric function and corresponding loss function ( $-\text{Im}\epsilon^{-1} = -v \text{Im}\chi$ ) along the  $c$  axis, which should be directly probed by inelastic scattering experiments of electrons or x rays [21], are shown over a broad energy range in Fig. 1. The wide structure [22] at  $\omega \sim 20$  eV in the loss function is the conventional plasmon corresponding to a density of  $\sim 8$  electrons per unit cell ( $r_s \sim 1.8a_0$ ). It suffices to note the correspondence between the near vanishing of the dielectric function and

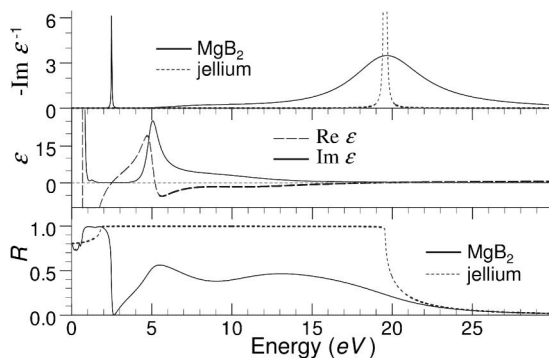


FIG. 1. Calculated loss function (upper panel), dielectric function (middle panel), and reflectivity  $R$  (lower panel), as well as the jellium counterparts (dashed lines) for  $q = 0.12 \text{ \AA}^{-1}$ , along the  $c$  axis.

the peak line shape of the loss function, illustrating the collective nature of this overdamped mode.

The most striking feature of the loss function shown in Fig. 1 is the sharp peak that occurs at  $\sim 2.45$  eV. The origin of this peak is evidently the prominent absorption at 5 eV in  $\text{Im}\epsilon$ , whose physics will be addressed shortly. Indeed, the strength of this charge fluctuation (notice the vertical scale of  $\epsilon$ ) is large enough to generate, through screening, an additional zero in  $\text{Re}\epsilon$ —thereby inducing a new collective mode. The extremely long lifetime ( $\Delta\omega < 10$  meV) of this mode is a consequence of both the strong dynamical screening in the vicinity of its energy, as reflected in the large slope of  $\text{Re}\epsilon$  [20,23], and the lack of particle-hole decay channels, courtesy of the large energy gap to be discussed below.

This additional collective excitation has a dramatic physical impact on the reflectivity, as shown in the bottom panel of Fig. 1. When possessing enough energy to excite this mode, the incident light suddenly penetrates the surface of the material with no reflection, much more abruptly than the case of a normal metal with a plasmon.

The reduction of reflectivity also provides a natural qualitative explanation for the large enhancement of the Raman efficiency [24] in a recent 2.41 eV Raman scattering study [9] of the  $E_{2g}$  phonon, as more photons are allowed to enter the surface to interact with the system.

Examination of the band structure, shown in the left panel of Fig. 2, reveals that the 5 eV structure in  $\text{Im}\epsilon$  originates mainly from the interband transitions between parallel bands. These transitions are facilitated by the strong [0002] crystal potential, which reflects the layered structure of this system and gives a large 5 eV gap (indicated by the arrows) at the  $\Gamma$  point. Intriguingly, as shown in the right panel of Fig. 2, where the real-space charge distribution of states marked by the down and up arrows is

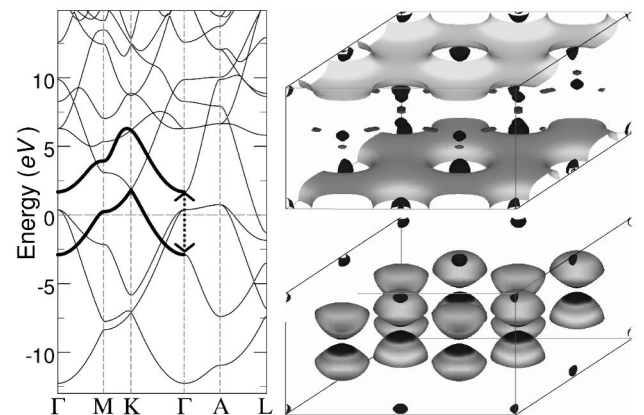


FIG. 2. Calculated band structure and density. The arrows in the band structure (left panel) indicate the large 5 eV gap between parallel bands. The isosurfaces of density for states marked by the upper/lower arrows are shown in the upper/lower right panel, which contains  $2 \times 2 \times 1$  unit cells with Mg in the corners.

illustrated, the states involved in the transitions reside in different planes and correspond to a B  $p_z$   $\pi$ -state and a layered conducting state of Mg  $s$  symmetry. Evidently, the above-mentioned additional mode consists of *coherent* charge fluctuations between B and Mg sheets, under the strong dynamical screening of low-energy intraband transitions [25].

Note that this mode is of very different nature from the  $d$  plasmon observed in a few post-transition metals. The  $d$  plasmon consists of *direction-insensitive* collective *dipole-like* oscillation of the *localized* electrons, originating from transitions of flat  $d$  bands to a *wide* range of final states. Thus, the corresponding absorption in  $\text{Im}\epsilon$  is usually 5–10 times smaller than the current case.

The wave vector dependence of the new collective mode, controlled by the competition between dynamical intraband screening and interband charge fluctuation, is shown in Fig. 3, in which the surface illustrates underlying single-particle transitions given by  $\text{Im}\epsilon(q \parallel [0001], \omega)$ . The first branch at  $\omega \sim 0.5$  eV of the low-energy ridge of the surface corresponds to the intraband charge fluctuation of the heavy carriers ( $p_{x,y}$   $\sigma$ -bands) to be discussed below, and the second branch to the light carrier ( $p_z$   $\pi$ -bands), while the high-energy ridge demonstrates the 5 eV interband transition. In the valley between these two main structures, where the phase space for single-particle excitation is closed due to the [0002] crystal potential, lies the weakly dispersed, induced collective mode (marked by dots), which eventually decays into electron-hole pairs of the light carriers at  $q \sim 0.6 \text{ \AA}^{-1}$ .

It is natural to wonder about the impact of this additional mode on the superconductivity, through reduction of the Coulomb pseudopotential,  $\mu^*$ . Within the static approximation adopted by previous authors [11,12], this new mode is found to have almost no effect on the static

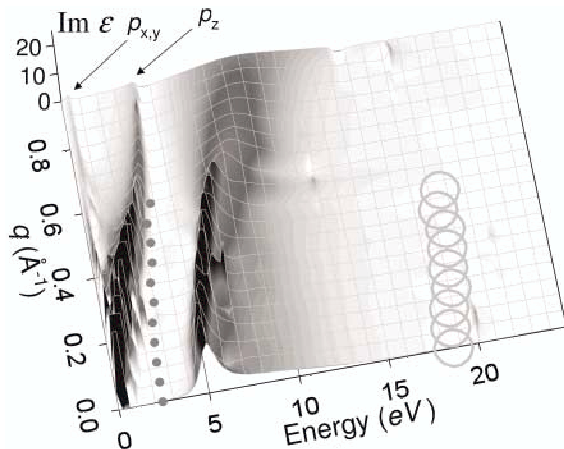


FIG. 3. Dispersion of collective modes and the single-particle decay channel. The dispersion of the induced/nominal collective mode is denoted by dots/circles until it becomes difficult to identify the peak energy of the plasmon. The surface illustrates  $\text{Im}\epsilon(q, \omega)$  for  $\vec{q} \parallel [0001]$ .

screened interaction, due to its very sharp line shape and small spectral weight compared to the conventional plasmon. In fact, the static limit of our resulting screened interaction is almost identical to that obtained from the homogeneous electron gas, despite its highly anisotropic energy dependence. One thus would expect a  $\mu^*$  of “normal” magnitude, if it is evaluated from the screened interaction [26]. However, due to the strong  $k$ -dependence of the Fermi surfaces, even the very idea of treating the screening through a single Coulomb pseudopotential may not be adequate [cf. Eq. (2.26) of Ref. [12]].

Now we address the proposed [5] AP with calculated dielectric function for small momentum/energy, shown in Fig. 4. The two main peak structures in  $\text{Im}\epsilon$  are related to the unusual characteristic of the Fermi surface [3]. The peak of lower energy corresponds to the intraband charge fluctuation of the heavy carriers, while the main peak results from the light carriers. More specifically, for a small momentum transfer  $q$  along the  $c$  axis, the cylindrical  $p_{x,y}$   $\sigma$ -hole Fermi surfaces [3] contribute to smaller energy (heavier mass), compared to the three-dimensional  $p_z$   $\pi$ -hole and  $\pi$ -electron Fermi surfaces. This double-peak structure is precisely what led to the suggestion of the AP [5], as the plasmon energy of the heavy carriers might be greatly screened by the light carriers and reduced to the upper edge of low-energy peak, whose energy increases linearly with small  $q$ .

However, this simple picture neglects electron-hole decay channels and the relative strength (or spectral weight) of these two carriers. As shown in Fig. 4, for small  $q$  there is a large supply of charge fluctuations ( $\text{Im}\epsilon \gg 1$ ) involving the light carriers at the upper edge of the low-energy peak. As a result, any collective mode of this energy would rapidly decay into electron-hole pairs (Landau damping) and have a negligible lifetime. In fact, our analysis suggests that a gap in the light-carrier bands at the Fermi energy is needed to allow an AP to exist. Furthermore, in this energy range,  $\text{Re}\epsilon$  is considerably larger than unity, reflecting the fact that the spectral weight from the heavy carriers is insignificant compared to the strength of

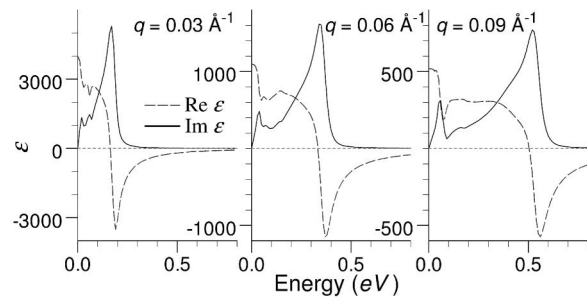


FIG. 4. Calculated dielectric function of  $\text{MgB}_2$ , for small  $q$ 's along the  $c$  axis. The low/high-energy peaks of  $\text{Im}\epsilon$  correspond to charge fluctuation of the heavy/light carriers. Note the large difference in the spectral weight and that  $\text{Re}\epsilon \gg 1$  between these two main structures.

the screening from the light carriers. In short, the potential acoustic plasmon is totally screened out and should not contribute to  $\mu^*$ . (The low-energy intra- $\sigma$  transitions may still lead to nonadiabatic corrections to the high energy, small  $q$  phonons, in particular the  $E_{2g}$  modes, which are most important for superconductivity.)

This kind of interplay between these two structures in  $\epsilon$  cannot be faithfully estimated by just counting the phase space, as performed in Ref. [5] with parametrized tight-binding bands. Instead, a careful evaluation of the corresponding transition probability, controlled by the matrix elements in Eq. (2), is necessary. The commonly made approximation of unit probability risks promoting unphysical charge fluctuations in the calculation, especially in the case of multiband models [27].

For a similar reason, the recently proposed two-band-type superconducting instability [7] in  $\text{MgB}_2$  is also not supported by our results. For  $q \sim (0, 0, \pi/c)$ , where the nesting between B  $\pi$ -electron and  $\pi$ -hole Fermi surfaces becomes “perfect,” there is no apparent enhancement at zero energy in our dielectric functions ( $q \sim 0.9 \text{ \AA}^{-1}$  in Fig. 3), contrary to the large interband polarizability obtained in Ref. [7]. Even though the formalism adapted in this work is different from that in Ref. [7], based on the experience gathered in the past years [19,20], we are confident that our results should not suffer from qualitative error for a simple  $sp$  system like  $\text{MgB}_2$ . Thus, the enhancement of interband pair scattering in Ref. [7] is an artifact of omitting the transition probability [cf. Eq. (9) of Ref. [7]] as discussed above.

In conclusion, a novel sharp collective mode, involving coherent charge fluctuation between B and Mg sheets, is predicted. This additional collective mode has a great impact on the optical properties of the material—suddenly switching off the reflectivity in the corresponding energy. It thus naturally explains the strong increase in the reported Raman efficiency at 2.41 eV, by increasing the chance of interaction. By contrast, the recently suggested AP is not supported by careful evaluation of the dynamical density response function, with the full information of all-electron KS band structure. The weak charge fluctuation from heavy carriers is totally screened out by the light carriers. Thus, the AP is effectively ruled out as a possible mechanism that brings an anomalously small Coulomb pseudopotential,  $\mu^*$ . Our results further demonstrate the importance of inclusion of realistic crystal potential effects, through the band dispersions (gaps) and matrix elements, in the calculation of charge fluctuation for systems with nonspherical Fermi surfaces.

This work was supported by DOE Grant No. DE-FG03-01ER45876 and an Accelerated Strategic Computing Initiative grant through Lawrence Livermore National Laboratory. A. G. E. and R. T. S. acknowledge support from NSF and NERSC.

- [1] J. Nagamatsu *et al.*, *Nature (London)* **410**, 63 (2001).
- [2] J. M. An and W. E. Pickett, *Phys. Rev. Lett.* **86**, 4366 (2001).
- [3] J. Kortus *et al.*, *Phys. Rev. Lett.* **86**, 4656 (2001); S. V. Shulga *et al.*, *cond-mat/0103154*; T. A. Callcott *et al.*, *Phys. Rev. B* **64**, 132504 (2001).
- [4] Y. Kong *et al.*, *Phys. Rev. B* **64**, 020501(R) (2001); S. Haas and K. Maki, *cond-mat/0104207*; P. Ravindran *et al.*, *cond-mat/0104253*; A. Y. Liu *et al.*, *Phys. Rev. Lett.* **87**, 087005 (2001).
- [5] K. Voelker *et al.*, *cond-mat/0103082*.
- [6] A. S. Alexandrov, *cond-mat/0104413*.
- [7] K. Yamaji, *J. Phys. Soc. Jpn.* **70**, 1476 (2001).
- [8] S. L. Bud'ko *et al.*, *Phys. Rev. Lett.* **86**, 1877 (2001); M. Imada, *cond-mat/0103006*; N. Kristoffel and T. Ord, *cond-mat/0103536*.
- [9] H. Martinho *et al.*, *cond-mat/0105204*.
- [10] J. Bardeen *et al.*, *Phys. Rev.* **108**, 1175 (1957).
- [11] G. M. Eliashberg, *Zh. Eksp. Teor. Fiz.* **38**, 966 (1960); P. B. Allen and R. C. Dynes, *Phys. Rev. B* **12**, 905 (1975).
- [12] D. J. Scalapino *et al.*, *Phys. Rev.* **148**, 263 (1966).
- [13] N. E. Bickers *et al.*, *Int. J. Mod. Phys. B* **1**, 687 (1987).
- [14] D. Pines, *Can. J. Phys.* **34**, 1379 (1956); B. N. Ganguly and R. F. Wood, *Phys. Rev. Lett.* **28**, 681 (1972); J. Ihm *et al.*, *Phys. Rev. B* **23**, 3258 (1981); G. S. Canright and G. Vignale, *Phys. Rev. B* **39**, 2740 (1989); G. D. Mahan and Ji-Wei Wu, *Phys. Rev. B* **39**, 265 (1989).
- [15] H. Fröhlich, *J. Phys. C* **1**, 544 (1968).
- [16] M. Petersilka *et al.*, *Phys. Rev. Lett.* **76**, 1212 (1996).
- [17] P. Blaha *et al.*, WIEN97.8, Technical University of Vienna, 1997; J. P. Perdew and Y. Wang, *Phys. Rev. B* **45**, 13 244 (1992).
- [18] The off-diagonal matrix elements in Eq. (2) incorporate the “crystal-local fields,” whose effect turns out to play a minor role in the present work.
- [19] A. G. Eguiluz, Wei Ku, and J. M. Sullivan, *J. Phys. Chem. Solids* **61**, 383 (2000); A. A. Quong and A. G. Eguiluz, *Phys. Rev. Lett.* **70**, 3955 (1993); N. E. Maddocks *et al.*, *Europhys. Lett.* **27**, 681 (1994); F. Aryasetiawan and O. Gunnarsson, *Phys. Rev. Lett.* **74**, 3221 (1995).
- [20] Wei Ku and A. G. Eguiluz, *Phys. Rev. Lett.* **82**, 2350 (1999), and references therein.
- [21] J. Fink, *Unoccupied Electronic States*, edited by J. C. Fuggle and J. Inglesfield (Springer, Berlin, 1992), p. 203; J. P. Hill *et al.*, *Phys. Rev. Lett.* **77**, 3665 (1996).
- [22] Fine structures in the plasmon line shape (e.g., a dip in the center) are suppressed for the ease of visualization.
- [23] K. Sturm and L. E. Oliveira, *Phys. Rev. B* **24**, 3054 (1981).
- [24] S. D. Sarma and D.-W. Wang, *Phys. Rev. Lett.* **83**, 816 (1999); M. Cardona, *Physica (Amsterdam)* **318C**, 30 (1999).
- [25] This additional mode can also be interpreted roughly as “zone-boundary collective state” if that concept is extended to cases with ionic anisotropic bonds; K. Sturm and L. E. Oliveira, *Phys. Rev. B* **30**, 4351 (1984).
- [26] K.-H. Lee *et al.*, *Phys. Rev. B* **52**, 1425 (1995).
- [27] Our work employs no pseudopotential which may introduce inaccuracy in evaluating the matrix elements. B. Adolph *et al.*, *Phys. Rev. B* **63**, 125108 (2001); J. M. Sullivan and A. G. Eguiluz (to be published).